ILAKAKA'S PINK SAPPHIRE CONUNDRUM: Statistical Analysis of υ^3 Antisymmetric Stretching in Zircon (SiO_4) as a Thermal History Indicator

High quality pink sapphire production is currently dominated by Ilakaka, Madagascar. The use of the full width half maximum (FWHM) of the υ^3 antisymmetric stretching in zircon inclusions in pink sapphire as a low-heat treatment detection is becoming an increasing topic of discussion as a criterion for this provenance. Therefore, characterizing zircon inclusions in Ilakaka, Madagascar pink sapphire before and after heat treatment in a controlled environment will hopefully help laboratories develop statistically relevant criteria for low-heat treatment detection. This study shows that after low-heat treatment (800°C for 2 hours), the color of most of the sapphires improved toward a purer pink. Visual alterations of monazites and micas were observed in 19% of cases. Fourier transform infrared spectroscopy (FTIR) was also used to detect the effects of low-heat treatment in 45% of cases. Raman spectroscopy was used to measure and quantify the υ^3 peak position and the FWHM of zircon inclusions before and after heat treatment. Results show that, on average, it decreased by 0.74 cm^{-1} while its peak position shifted toward lower numbers by an average of 2.49 cm^{-1}. This study also shows that the interpretation of the Raman spectra of zircons includes an astonishing amount of false positives as well as false negatives. Interestingly, its use in zircon inclusions surrounded by tensions may be used to identify the unheated tensions due to a metamict process versus tensions resulting from the thermal expansion of the treatment.

By Martial Curti, Hugo Ellia, Dr. Giada Musilli, Theodore Rozet, Valentin Fejoz, Carolina Guzzi, Piotr Hinnemann, and Elsa Marlin

Ilakaka sapphires present a particularly challenging authentication for gemological laboratories worldwide as a result of the area's dominant place as a producer of high-quality pink sapphires in the market, combined with the gem's chemistry that enables a very good color change after low temperature heat treatment: from violet and purple hues to a more valuable pink (Figure 1). Lastly, Ilakaka sapphires contain, for the vast majority, only protogenetic zircon inclusions (with trace amounts of radioactive elements). This last point is important because, in gemological science, the surrounding tension resulting from thermal expansion between an inclusion and its host is a key visual factor in heat treatment detection (Dunaigre., 2006; Pardieu et al., 2015). However, a solid inclusion undergoing a metamictization will, over time, expand and may create a surrounding tension as well (Saeseaw et al., 2020). Therefore, a gemologist confronted with such a scenario, with all other gemological properties being equal, will interpret the tension subjectively. Recent times saw the rise of Ilakaka pink sapphires, whose scenario described above is no longer an oddity but a common issue faced by gem labs. Hence, the quest to find the best low-heat treatment detection focuses on the zircons (Karempelas et al., 2023; Saeseaw et al., 2019., Krzemnicki., 2018., Wang et al., 2006).

Figure 1. A 1.25 ct pink sapphire from Ilakaka, Madagascar before and after low-heat treatment. (Photo: M.P.H. Curti/Bellerophon Gemlab, reference collection No B76311)

In Brief

- Raman spectroscopy may be of use to separate unheated metamict tensions from thermal ones.
- Careful observation, coupled with Raman spectroscopy, and FTIR enable treatment detection with 97% accuracy.

Materials and Methods

Samples and Instruments. Thirty-three samples, collected directly from the mine in Ilakaka, Madagascar in December 2022 by our team, were selected and polished with two windows for data analysis, thickness sizes ranging from 0.44 mm to 3.10 mm. Sample sizes ranged from 0.38 to 2.53 ct. All samples were selected based on their colors: pink to purple and the prominent presence of hydroxides: kaolinite and/or boehmite in their Fourier transform infrared (FTIR).

To compare the true color of the samples before and after treatment, we used a Canon EOS 2000D camera with a Sigma Macro DG 105-mm lens to produce consistent results. Photographs were taken under identical lighting conditions, with the samples placed in a Pantone Light Booth (5000 K lamp).

Color analysis (Table 1) was performed on an integrating sphere with a diameter of 50 mm with a typical reflectance of 99% in the visible range, using an SR-4XR250-50 Ocean Insight spectrometer 500 lines blazed at 250 nm, with a slit 50, coupled with a pulsed Xenon 220 Hz, 220 -750 nm, and a halogen light source.

Photomicrographs of internal inclusions were captured at Bellerophon Gemlab under different magnifications with a Keyence VHX-6000 system and under different types of illumination, together with a fiber optic light source.

Non-polarized FTIR spectra were collected at Bellerophon Gemlab using a Frontier Perkin Elmer FTIR spectrometer equipped with a 4X beam condenser accessory and a diffused reflectance (DRIFT). The resolution was set at 4 cm^{-1}. Infrared spectra were collected in multiple areas and of each sample before and after heat treatment.

Raman spectra were obtained at Bellerophon Gemlab using a BWT-8400000340 i-Raman Plus 785S. For internal inclusion analysis, the system was operated in confocal mode with 20X and 50X objectives using a 785 nm highly coherent laser.

Photoluminescence spectra were also collected at Bellerophon Gemlab, using a SR-4XR250-50 Ocean Insight spectrometer 500 lines blazed at 250nm, with a slit 50, coupled with a 250 nm excitation LED light source.

Short wave ultraviolet photographs were taken using a Canon EOS 2000D camera with a Sigma Macro DG 105 mm through a short-pass filter, with a cut-off wavelength at 600 nm in a black box illuminated by a 253.4 nm light source.

Table 1. Color-calibrated photos and color analysis of 15 samples before heating and after heating.

Sample ID	Before Heating	After Heating	Before Heating	After Heating
T0325				
T0326				
T0327				
T0328				
T0329				
T0330				
T0332				
T0334				
T0336				
T0337				
T0338				
T0340				
T0342				
T0343				
T0344				

Heating experiment. The 33 pink sapphires were first subjected to a gentle heat to mimic the doping part of the cutting process, then subjected to heat treatment in air at 800°C for 2 hours in order to study, at each step, the effect on color, inclusions, infrared spectroscopy, fluorescence, and the change in zircon inclusions using Raman spectroscopy.

Samples were first placed individually on a tweezer at 3 cm from the tip of the flame of an alcohol lamp for 18 to 34 seconds. The length of time a sample was subjected to the candle is based on actual measurement of the doping time in cutting factories times 2 (as doping is done a minimum of two times). Measurement of temperatures ranging on average to 350°C was made using two thermocouples: one placed directly in contact with the sample; the other offset at 1 cm from the sample. Lastly, the temperatures of the samples were also regularly measured using an infrared non-contact thermometer.

Thirty-one samples were then placed on an alumina ceramic plate (99.9% Al_2O_3) in a 1950°C-muffle furnace and heated to 800°C at a rate of 30°C/min with the door open. At the end of the heating cycle, the furnace was switched off. The samples were removed and allowed to cool to room temperature.

Results and Discussion

Color Appearance. Almost all samples had their color improved to a purer pink through the reduction of the blue color component from the intervalence charge transfer of Fe^{2+} and Ti^{4+} ions (Dubinsky et al., 2020) due to the oxidation treatment (Figure 2). Interestingly, some samples gained a reddish tone, most probably due to phase transformation of the orange epigenetic iron oxides present in those samples (Sripoonjan et al., 2016).

Fluorescence. Photoluminescence and fluorescence analyses focused on the chalky white fluorescence emission at 410 to 480 nm (Wong, et al., 1995) due to charge transfer between O^{2-} and Ti^{4+} ions (Emmett et al., 2017) observed in heated sapphire. The result shows no visual observation of chalky white fluorescence and no emission in the blue using our current system before and after treatment.

Internal Features. ***Visual Observations.*** The 33 samples contain numerous rounded protogenetic zircons, 42% of the unheated sapphire references presented zircons with tension halos like discoid fractures surrounding at least one zircon, that developed from its expansion

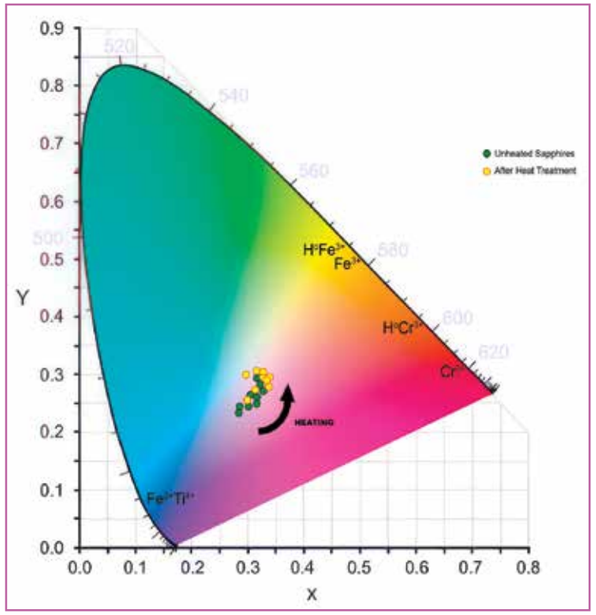

*Figure 2. CIE-L*ab Color analysis before and after heat treatment.*

Figure 3. Tension halo developed by radiation damage accumulation over time.

due to the radiation damage accumulation (Figure 3) (Saeseaw et al., 2020). While 24% of the pink sapphires generated at least one tension surrounding zircons after heat treatment due to thermal expansion (Figure 4), 2% of the zircons changed to a translucent frosty appearance, most probably due to partial melting of the zircons (Wang et al., 2006; Wanthanachaisaeng, 2007). Mica is present in 9% of the samples with two samples presenting mica with discoid fracture after

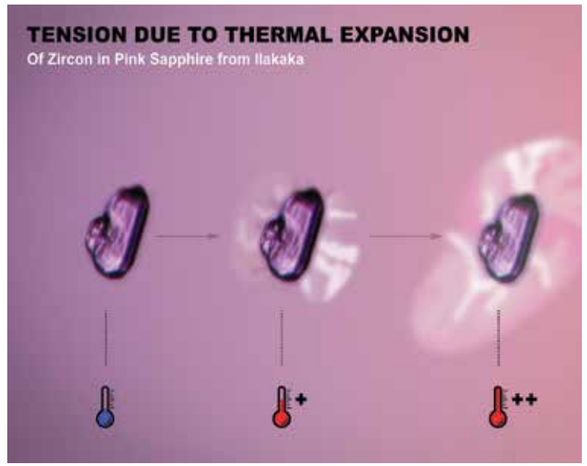

Figure 4. Tension halo developed by low-heat treatment.

heat treatment. Monazite is present in 10% of the samples as well. Initially brown, all monazites lost their color after treatment, confirming previous studies as a good indicator of heating when near colorless (Saeseaw et al., 2020).

Infrared Spectroscopy. ***Focus on Hydroxides.*** In this study, we selected pink sapphires with an obvious presence of Kaolinite and/or Boehmite. Of the 33 samples, 64% completely lost the hydroxide presence in their spectra after the gentle heat used for the doping process at ~350°C for few seconds, while no trace of hydroxides remained in any references after the heat treatment at 800°C in air for 2 hours (Figure 5).

Focus on the 3309 cm^{-1} and 3275 cm^{-1}. Of all the samples, 88% displayed the presence of a 3309 cm^{-1}, associated with OH stretching and titanium ions in pairs (Balan, 2020). All references showed a decrease in the absorbance of their 3309 cm^{-1} after heat treatment (Table 2) in accordance with a previous study (Saeseaw et al., 2020), while 15% displayed a 3275 cm^{-1} visible after the disappearance of the hydroxide in unheated samples only, also in accordance with a previous study (Krzemnicki, 2018).

Focus on the 3232 cm^{-1} and the 3184 cm^{-1}. Numerous studies (Saeseaw et al., 2020; Pardieu et al., 2015; Saeseaw et al., 2018; Krzemnicki, 2018) have shown the importance of the 3232 cm^{-1} and the 3184 cm^{-1}, both associated with OH stretching and isolated titanium ions (Balan, 2020) as an indication of heating in non-basalt related corundum. 45% of the samples developed a

Table 2. Results of the 3309 cm-1 height before and after heating.

3309 cm^{-1} Peak height	Unheated		Heated	
	Samples	Percentage	Samples	Percentage
0 to <0.001	4	12%	20	65%
0.001	2	6%	5	16%
0.002	4	12%	3	10%
0.003	12	36%	3	10%
0.004	6	18%	0	0%
0.005	2	6%	0	0%
0.006	1	3%	0	0%
0.007	0	0%	0	0%
0.008	2	6%	0	0%

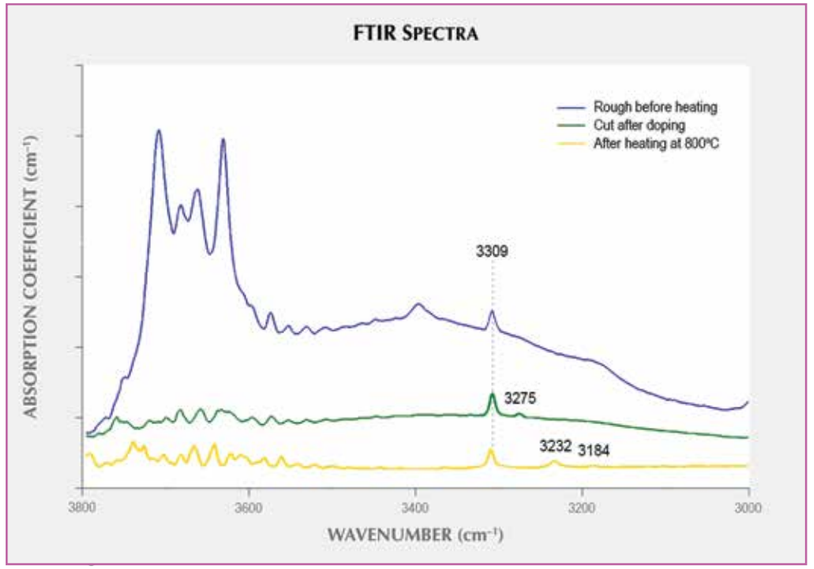

Figure 5.Comparison of representative non-polarized unoriented FTIR spectra of pink sapphires from Ilakaka, Madagascar; rough before (blue) and after (green) gentle heating at ~350°C for a few seconds, as well as after heating at 800°C for 2 hours (yellow). Spectra are offset vertically for clarity.

3232 cm^{-1}, while 16% displayed a 3184 cm^{-1} after heat treatment (Table 3). In accordance with gemological literature, the samples not presenting a 3309 cm^{-1} in their unheated states did not develop a 3232 cm^{-1} or a 3184 cm^{-1} after heating (Saeseaw et al., 2020; Pardieu et al., 2015; Saeseaw et al., 2018).

As the cause, the detection and understanding of the 3232 cm^{-1} has already been widely discussed and is not the focus of this study. It is nevertheless important to note that it remains, based on the 33 samples, the most accurate indication of low-temperature heating in non-basalt related corundum. The samples are small in size, with the 3232 cm^{-1} detection correlated to a sample volume, suggesting an increased detection in a day-to-day operation (Beran., 1991).

Table 3. Qualitative results of FTIR before and after heating.

FTIR Absorbance (cm-1)	Unheated (cut)		Heated	
	Samples	Percentage	Samples	Percentage
Hydroxide(s)	12	36%	0	0%
3309	29	88%	18	58%
3275	5	15%	0	0%
3232	0	0%	14	45%
3184	0	0%	5	16%

Raman Spectroscopy. It is well known that the Raman spectra of v^3 at ~1010 cm^{-1} related to SiO_4 vibration modes is the most sensitive to radiation damage accumulation, quantifiable through the full width at half of its maximum of its peak (Figure 6) (Holland et al., 1955). It is also assumed that most Pan-African Orogeny zircons contain radioactive trace elements (Hanchar and Hoskin, 2003; Elmaleh et al., 2019; Garver, 2002). The radioactive decay of these uranium and/or thorium trace elements creates disorder within the zircon structure over time.

Most metamorphic gemstones found within Ilakaka are believed to be formed somewhere around 565 to 490 million years ago (Rakotondrazafy et al., 2008). Indirectly through the interpretation of the degrees of a zircon inclusion structural state, gemologists may derive the unheated sapphire's host provenance between countries of origin that are separated by important time scales (Xu and Krzemnicki, 2021). We have also known for a long time (Pabst, 1952) that the metamict process is reversible by heat whose energy re-orders a zircon structural state (Meldrum et al., 1998) up to ~1400°C. Past this point, zircon in sapphire starts to decompose into its oxide components without melting: baddeleyite – ZrO_2 and SiO_2 – rich phase (Wang et al., 2006).

Focus on unheated zircon. Of the 33 samples in their unheated states, we collected the Raman spectra of 128 zircon inclusions. The lowest full width half maximum found (FWHM) is at 6.57, while the highest FWHM is 19.89. The average is 11.01, and the median value is at 10.41 FWHM (Table 4). The maximum FWHM deviation between zircons in the same sapphire is 9.33 while the lowest deviation stands at 0.59, with an average of 3.58 deviation and a median deviation value at 2.87 based on 103 zircons found in 28 pink sapphires from Ilakaka. The lowest peak position of v^3 is 1006.05 cm^{-1}, while the highest one is at 1020.18 cm^{-1}. The average v^3 position is at 1013.21 cm^{-1} and the median stands at 1013.06 cm^{-1}. The maximum v^3 peak deviation within a sapphire is 7.71 cm^{-1}, while the lowest deviation stands at 0.29, with an average of 2.27 deviation and a median deviation value at 1.94.

Focus on heated zircon. Of the 31 samples from their heated states, we collected the Raman spectra of 125 zircon inclusions. The lowest FWHM found is at 6.11, while the highest FWHM is 18.55. The average is 10.27 (Table 4), and the median value is at 10.06 FWHM. The maximum FWHM deviation between zircons in the same heated sapphire is 10.36 while the lowest deviation stands at 0.52, with an average of 4.37 deviation and a median deviation value at 3.74 based on 123 zircons found in 29 pink sapphires from Ilakaka. The lowest peak position of v^3 is 1005.64 cm^{-1}, while the highest one is at 1017.04 cm^{-1}. The average v^3 position is at 1010.72 cm^{-1} and the median stands at 1010.75 cm^{-1}. The maximum v^3 peak deviation within a sapphire is 8.35 cm^{-1}, while the lowest deviation stands at 0.03, with an average of 2.75 deviation and a median deviation value at 1.87.

It is important to note that the zircons analyzed before and after heat treatment in Table 4 may not be the exact same ones, as some samples displayed numerous zircon inclusions (some more than 50). (To see the effect of heat on a single zircon, see below.) However, it is the authors' belief that the spectra of these 253 zircons provide a good representation of what gemologists find when performing Raman spectroscopy on v^3 in zircon inclusions inside a pink sapphire from Ilakaka, Madagascar. We may add that these results conform to what we see on a day-to-day basis, as well as in concordance with previous studies (Karempelas et al., 2023; Saeseaw et al., 2019; Krzemnicki, 2018; Wang et al., 2006; Wanthanachaisaeng, 2007).

Focus on Raman spectra interpretation. The peak position of v^3 as well as its FWHM is affected by the zircon uranium concentration, its surrounding

Table 4. Results of Raman analysis of zircon inclusions, reported in average ± SD (n = number of analyzed sapphires).

References Samples	Unheated (n=33)		Heated (n=31)	
	Peak Position (cm^{-1})	Measured FWHM (cm^{-1})	Peak Position (cm^{-1})	Measured FWHM (cm^{-1})
T0325	1016.68 ± 0.24	12.32 ± 1.25	1011.64 ± 1.43	12.09 ± 0.57
T0326	1012.86 ± 1.64	11.78 ± 0.78	1010.23 ± 1.20	11.28 ± 0.52
T0327	1016.86 ± 0.86	9.55 ± 0.32	1010.83 ± 0.89	12.27 ± 0.51
T0328	1014.34 ± 1.24	10.60 ± 2.34	-	-
T0329	1013.26 ± 1.10	9.22 ± 2.46	1011.38 ± 2.02	10.11 ± 2.93
T0330	1011.07 ± 0.85	9.19 ± 0.72	1009.46 ± 0.74	9.18 ± 0.79
T0332	*1013.00*	*10.00*	1010.22 ± 0.01	9.66 ± 0.29
T0334	1010.31 ± 3.41	13.91 ± 1.83	1009.02 ± 2.26	11.29 ± 2.71
T0336	1013.50 ± 0.50	13.14 ± 0.32	1010.12 ± 2.90	11.72 ± 2.75
T0337	1012.23 ± 1.37	10.08 ± 1.23	1010.71 ± 0.51	9.45 ± 0.87
T0338	1014.60 ± 1.80	11.01 ± 0.83	1011.65 ± 0.38	10.56 ± 1.08
T0339	*1013.56*	*15.13*	-	-
T0340	1014.06 ± 0.74	10.69 ± 0.62	1012.82 ± 2.89	12.75 ± 2.44
T0342	1012.32 ± 0.65	16.86 ± 1.05	1009.89 ± 0.98	11.62 ± 1.17
T0343	1016.00 ± 0.27	10.15 ± 0.30	1012.62 ± 0.20	11.20 ± 2.07
T0344	1010.99	9.97	1008.10 ± 0.42	11.21 ± 1.21
T0349	1012.26 ± 0.52	8.94 ± 0.63	1010.28 ± 0.68	7.66 ± 0.26
T0350	1012.60 ± 0.40	10.70 ± 2.89	1010.85 ± 1.03	9.34 ± 1.95
T0352	1013.77 ± 0.31	9.77 ± 0.82	1009.75 ± 2.32	9.22 ± 1.63
T0353	1012.73 ± 1.13	12.01 ± 1.89	1011.70 ± 0.94	9.69 ± 1.14
T0356	1012.67 ± 0.14	10.87 ± 0.54	1011.37 ± 0.07	9.99 ± 0.51
T0357	1012.47 ± 1.44	8.43 ± 0.98	1009.17 ± 0.83	11.34 ± 3.00
T0359	1011.25 ± 0.55	12.73 ± 3.18	1010.17 ± 0.52	9.06 ± 1.61
T0361	1012.81 ± 0.52	12.50 ± 2.31	1011.03 ± 0.42	9.17 ± 2.05
T0362	*1006.60*	*12.41*	*1010.58*	*8.59*
T0366	1014.31 ± 2.04	12.35 ± 4.22	1012.05 ± 1.50	11.30 ± 1.79
T0368	1014.78 ± 0.27	9.87 ± 0.92	1011.16 ± 0.53	8.92 ± 1.44
T0370	1013.20 ± 1.07	12.41 ± 1.81	1011.26 ± 0.26	9.58 ± 0.94
T0373	1014.39 ± 0.78	9.93 ± 0.99	1011.7 ± 0.68	10.89 ± 4.44
T0376	1011.96 ± 0.72	9.33 ± 1.44	1012.47 ± 2.41	11.71 ± 3.57
T0380	1012.57 ± 0.81	11.14 ± 1.32	1011.08 ± 0.63	10.85 ± 2.15
T0386	1010.18 ± 0.51	9.11 ± 0.80	1009.65 ± 0.47	8.96 ± 0.54
T0389	*1015.38*	*7.63*	*1009.56*	*7.81*
Total	**1013.21 ± 0.92**	**11.01 ± 1.39**	**1010.72 ± 0.97**	**10.27 ± 1.51**

Italic for sapphire with only 1 zircon. (Not included in averages and SD)

pressure (Zhang, 1998), any heat it was subjected to, and its radiation damage as a function of the effective accumulation of time since its formation (Marsellos et al., 2010; Wanthanachaisaeng, 2007). The wide variations between zircons can be explained by the well-known variation in their uranium content, the diversity of pressures they are exposed to in a sapphire, influenced by the respective axis of the host in relation to the zircon (Ragan et al., 1992), and the sapphire formation, defects and chemistry, and the zircon defects and chemistry, their depths including the length of the laser path, their times of formation, and the variety of heat they have been subjected to during their geological life and/or due to treatment.

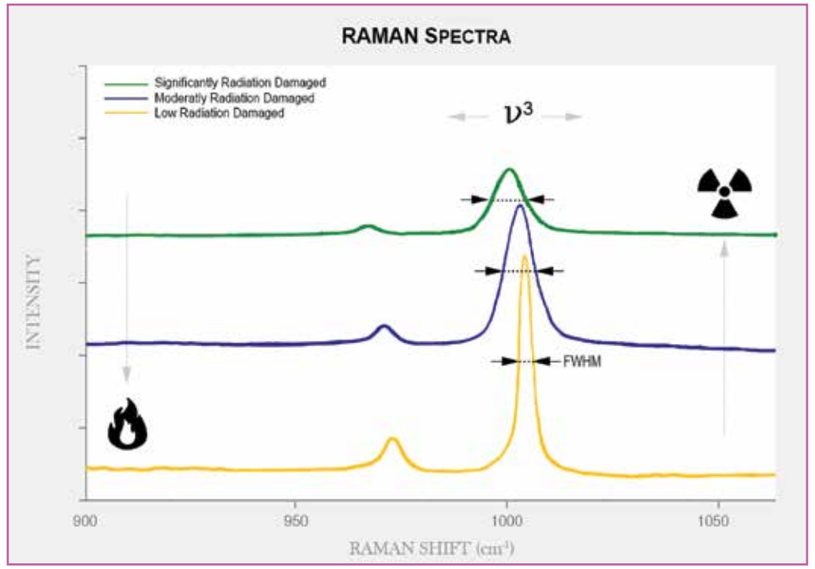

Figure 6. Representative stacked Raman spectra of zircon inclusions in sapphires from a well-ordered crystalline state to a significantly radiation-damaged one, as well as the reversible effect of radiation and heat. FWHM calculated by a software-integrated Gaussian-Lorentzian function after baseline correction. Spectra are offset vertically for clarity.

The Raman interpretation of zircon inclusions in pink sapphires from Ilakaka, Madagascar is widely used in laboratories as a routine test since it may provide supporting analytical evidence of heat treatment. However, cautions regarding its use as a conclusive criterion for low-heat treatment have been issued in numerous studies (Krzemnicki et al., 2021; Saeseaw et al., 2020; Wang et al., 2006). It is the authors' opinion that its interpretation may be at the root cause of numerous conflicting opinions regarding what is or what is not an indication of heating. The present study seeks to add its data to the previous research (Krzemnicki et al., 2021; Karampelas et al., 2023; Wanthanachaisaeng, 2007) while attempting to quantify the accuracy of such techniques as well as the numerous false positives and false negatives based on various factors and interpretations applied to the whole population of zircons analyzed and different case-by-case scenarios.

Focus on v^3 FWHM versus v^3 peak position. Of the 233 zircons analyzed (Figure 7), we see a noticeable and well known overall shift toward lower peak positions, most likely due to the reduction in pressure from the contraction of the zircon as a factor of the re-ordering of its structure, as well as the sapphire host expansion by the thermal energy input from the treatment (Wanthanachaisaeng, 2007; Zhang et al., 2000; Nasdala et al., 2002).

A similar well known overall shift toward a lower FWHM due to the healing of the zircon structural radiation damage from the heat treatment is distinguishable. However, the use of any values from the FWHM of v^3 provides very poor accuracy for low-heat treatment detection. Using an FWHM value of 10 yields a detection accuracy slightly higher than a coin toss, with 44% of heated samples in the unheated category, while 43% of unheated samples will fall under the heated one.

Using an FWHM value of 8, more than one stone out of 15 unheated ones will be misidentified as heated, and more than two-thirds of the heated samples will be undetected. Lastly, using a value of 6 provides the most interesting results with no false positives. Even with only one stone being correctly identified, different heating conditions such as increased temperature and/or time may pull the zircon's values further below this value, improving its potential use.

To increase the relevance of our study and minimize the influences of factors such as heating conditions, Raman spectrometer gratings, laser wavelength, and deconvolutions formulae used, we added the zircon values of previous studies (Figure 8). Of the 638 zircons plotted and more than 126 sapphires from Ilakaka, using an FWHM value of 10 yields a detection accuracy a little bit better than our values alone, with more than one heated stone for every five undetected, and almost one for every two unheated stones misidentified as heated. While an FWHM value of 8 misidentified more than one out of every 8 unheated zircons as heated, and more than two-thirds of heated as unheated, results are in accordance with the samples of the present study alone. Lastly, an FWHM value of 6 yields an acceptable low detection rate of more than one in every 10 heated stones correctly identified and false positives below 2% of an unheated one misidentified as heated.

Focus on v^3 FWHM deviation versus v^3 peak position deviation. The obvious inconvenience of v^3 deviation measurement is the need to have multiple reachable zircons in a sapphire, moreover, the more zircons the higher the chances of an increased deviation, discernible in the approximate linear correlation between the number of zircons in a sapphire with its deviations (Figure 9). As noted previously, it is distinguishable in Figures 7 and 8 that the deviations between zircons after heating seems to be reduced in terms of v^3 FHWM and peak position. However, results in Figure 9 show that the use of the zircon FWHM deviation within a sapphire yields even poorer low-heat treatment detection results.

Focus on v^3 FWHM versus v^3 FWHM deviation. The FWHM value compared to its deviation has been the subject of a recent article as a means to help detect low- heat treatment (Karampelas et al., 2023; Krzemnicki, 2023). Assuming the best-case scenario, where the minimum value is found within a sapphire in its heated state and compared against the minimum values recorded in unheated ones, more than one unheated stone out of every 15 will be misidentified as heated while 77% of heated will fall under the unheated category (Figure 10). The important deviation from zircons within a sapphire carries important practical implications for gemstones with numerous zircons. Laboratories may not analyze the same ones, while the same laboratories may be confronted with opposite results on a gemstone resubmitted. Lastly, a gemstone that would be recut may give completely different results based on the zircons removed and the ones that are left over (Figure 11).

It is also important to note the intrinsic repeatability issues of the quantification of v^3 FWHM within the same zircon. A zircon uranium's content is not homogenous throughout its structure (Krogh and Davis, 1975). As such, the same laboratory analyzing the same zircon may have widely fluctuating results based on the exact spot analyzed, the magnification used, as well as the path taken to analyze it, thus making its correct interpretation even more difficult (Figure 12).

Focus on tension genesis identification. Going back to the visual observations of the present study, it is the authors' belief that the root cause of most focus on zircon analysis in pink sapphire from Ilakaka is linked to the subjective interpretations of the tensions surrounding

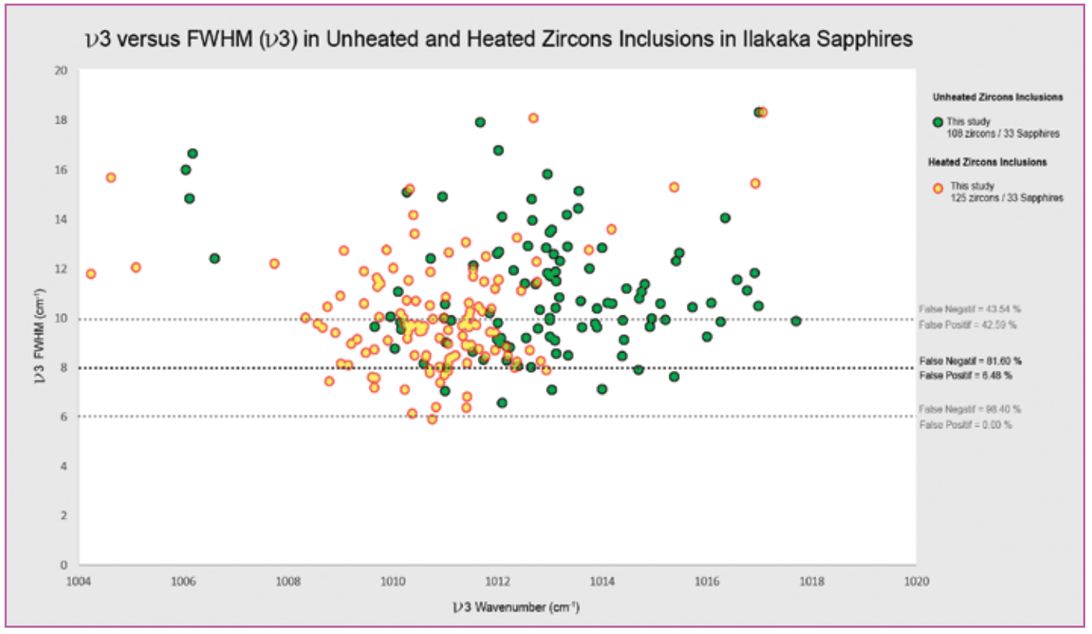

Figure 7. Among the 233 zircons plotted in this study, a perceptible shift toward lower FHWM, peak positions, and reduced deviation from unheated (green) to heated (yellow) is to be noted. However, the use of the FWHM alone at any value provides a very poor low-heat treatment detection accuracy.

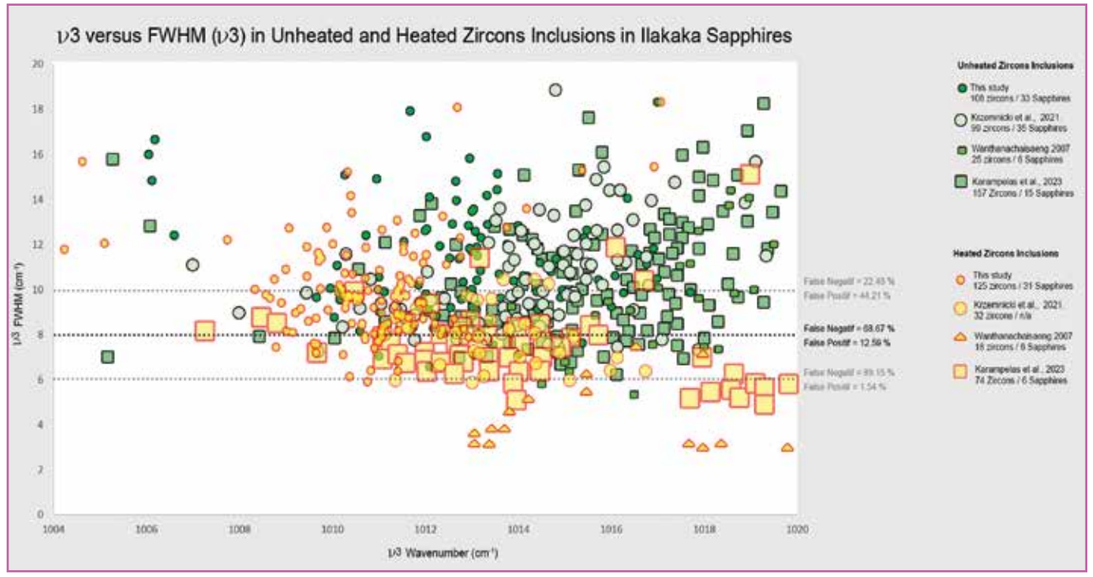

Figure 8. To increase the relevance of our study and minimize external factors, we plotted our reference group for a total of 638 zircons from three different precedent studies. We can notice that all results are fairly similar in their values from unheated (green) to heated (yellow).

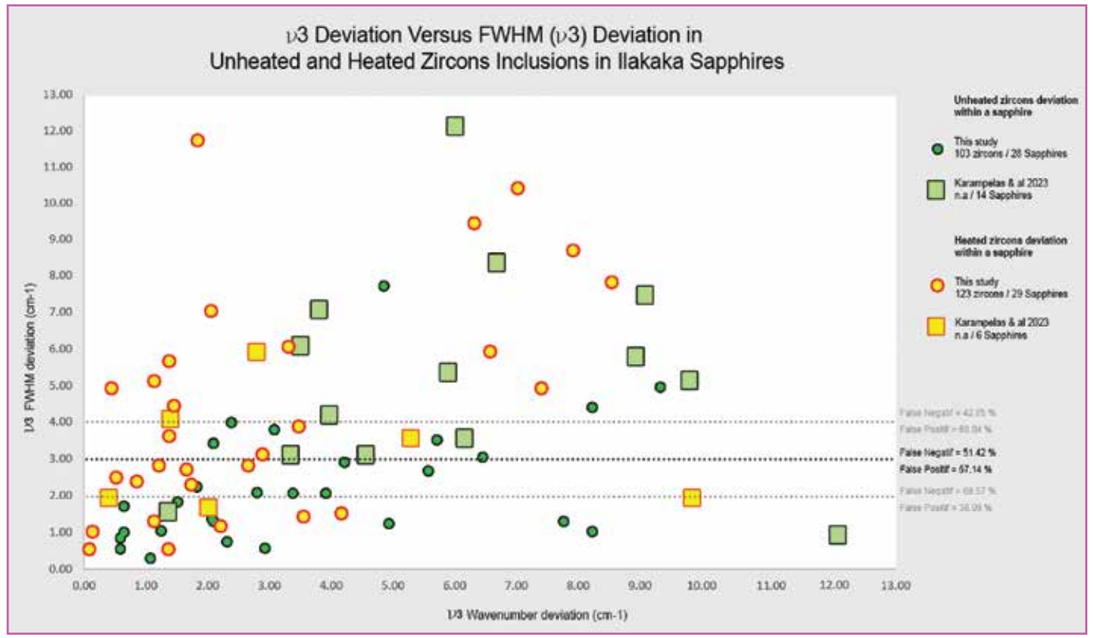

Figure 9. The deviations of zircon FWHM and peak position seem to have a higher correlation to the number of zircons present within a pink sapphire than its practical use as low-heat treatment detection.

a zircon (Figure 13). Therefore, we referenced the v^3 peak positions and the FWHM as carefully as possible, trying to follow the same laser path and targeting the same local area before and after heating of 20 zircons surrounded by tensions due to the metamictization process in their unheated state and in their heated state (Table 5). We also analyzed 7 zircons that developed tension after heat treatment only, assumed to be the result of thermal expansion (Table 6).

Based on these 20 references, no unheated metamict tensions presented an FWHM below 12. Their average peak position was at 1013.97 cm^{-1} and their median value was at 1014.66 cm^{-1}, with a standard deviation of 3.42. Their average FWHM was 15.47 and their median FWHM value was 14.55, with a standard deviation of 2.24, thus confirming the correlation between the radiation damage and the outward pressure needed to generate a tension displayed in the values of these samples being much higher than the control group.

The changes in the zircons with metamict tension values before and after heating are also much higher than the other references, with an average of 3.49 reductions in their FWHM compared to the previous 0.74. This suggests an exponential re-ordering of the zircon structure in relation to their amount of radiation damage that should be investigated further. We also note an important shift in the peak position toward lower numbers with an average of 3.63 cm^{-1}, suggesting a notable reduction in pressure after heat treatment. Lastly, the 7 zircons whose tension is due to the thermal expansion of the treatment present a lower average FWHM of 9.48 and a median FWHM value of 9.99, suggesting that, in these cases, the anisotropic expansion behaviors of both, inclusion and host, are an important factor in the generation of "thermal"

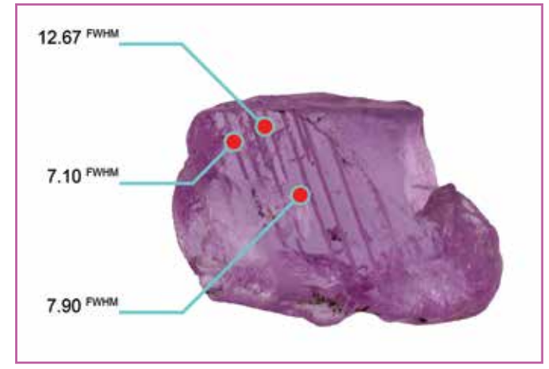

Figure 11. Sample T0329 in its unheated state, possibly misidentified as heated should the zircon with the FWHM of 12.67 be removed after its cut.

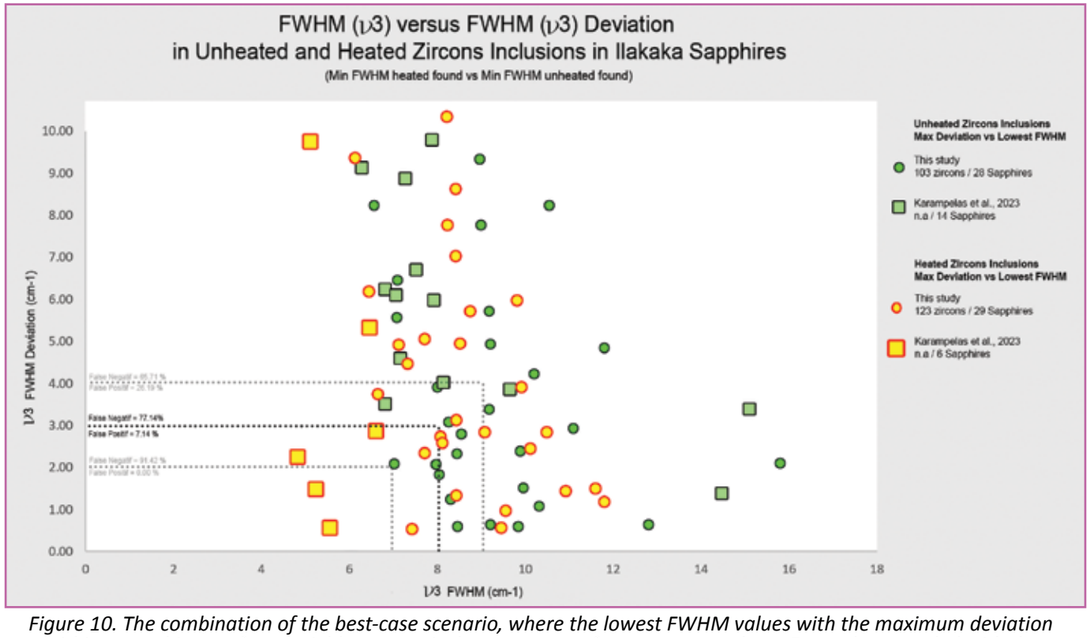

Figure 10. The combination of the best-case scenario, where the lowest FWHM values with the maximum deviation within a sapphire are found, yields no practical uses on our reference groups alone. Even when coupled with the previous study, its accuracy remains poor.

Table 5. Results of Raman analysis of zircon inclusions with metamict tension (n = number of analyzed zircons).

References Samples	Lighting: Darkfield	Lighting: Direct	Unheated (n=20): Peak Position (cm^{-1})	Unheated (n=20): Measured FWHM (cm^{-1})	Heated (n=14): Peak Position (cm^{-1})	Heated (n=14): Measured FWHM (cm^{-1})	Deviation (n=14): Peak Position (cm^{-1})	Deviation (n=14): Measured FWHM (cm^{-1})
T0325 a			1015.36	15.31	1009.66	11.49	5.70	3.82
T0325 b			1015.47	15.07	1011.49	12.19	3.98	2.88
T0325 c			1016.08	13.33	1011.71	11.69	4.37	1.64
T0326 a			1009.08	17.69	1009.20	11.97	-0.12	5.72
T0326 b			1011.21	14.14	1010.40	10.90	0.81	3.24
T0326 c			1019.00	18.01	1009.96	12.25	9.04	5.76
T0327 a			1020.18	13.18	1010.68	12.07	9.50	1.11
T0327 b			1016.68	13.62	1011.99	11.77	4.69	1.85
T0334 a			1006.10	18.31	1005.03	12.27	1.07	6.04
T0336 a			1014.36	13.50	1011.41	10.83	2.95	2.67
T0336 b			1008.16	19.59	1010.37	13.63	-2.21	5.96
T0338 a			1014.61	12.65	1012.22	10.49	2.39	2.16
T0338 b			1015.33	14.33	1011.97	11.75	3.36	2.58
T0342 a			1011.02	14.04	1008.70	10.66	2.32	3.38
T0328 a			1014.70	14.59				
T0328 b			1012.76	19.89				
T0328 c			1016.91	18.44				
T0328 d			1013.15	13.70				
T0328 e			1015.85	14.50				
T0328 f			1013.29	15.48				
Average			1013.97	15.47	1010.34	11.71	3.42	3.49
Median			1014.66	14.55	1010.54	11.76	3.16	3.06
SD			±3.42	±2.24	±1.82	±0.79		

Figure 12. The FWHM deviation within a zircon is due to its local uranium content, making the repeatability and reliability of such analysis even more difficult.

tensions. Corundum, with a thermal coefficient of expansion higher than the zircon at both the principal axis (a = 7.3 x 10^{-6} and c = 8.3 x 10^{-6} for corundum versus a = 3.4 x 10^{-6} and c = 5.6 x 10^{-6} for zircon) (Wanthanachaisaeng, 2007), may indicate a correlation between high crystalline zircons in their unheated state and the probability of generating a thermal tension during the treatment.

Analysis by micro-Raman spectroscopy of zircons surrounded by a discoid "halo-like" tension may provide useful indications regarding the genesis of the said tension, potentially important regarding the heat treatment history of the host. Only unheated metamict-generated tensions presented an FWHM superior to 14,

Table 6. Results of Raman analysis of zircon inclusions with thermal tensions, (n = number of analyzed zircons).

References Samples	Heated (n=7): Peak Position (cm^{-1})	Heated (n=7): Measured FWHM (cm^{-1})
T0330	1008.74	7.65
T0338	1012.22	10.49
T0344	1008.5	9.99
T0362	1010.58	8.59
T0373	1014.5	9.01
T0376	1010.16	10.19
T0380	1011.67	10.47
Average	1010.91	9.48
Median	1010.58	9.99
SD	±1.94	±1.01

Figure 13. Causes of discoid tensions surrounding a zircon in a sapphire.

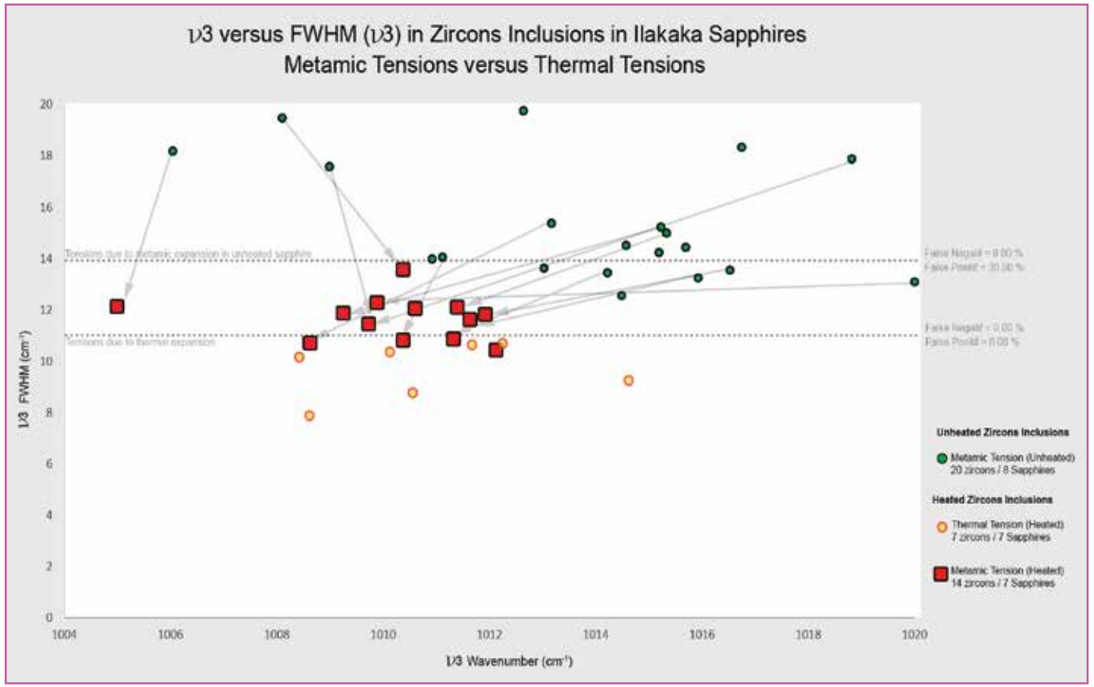

Figure 14. Metamict tension before treatment (green), after treatment (red), and thermal tension (yellow) display a much more important variation of structural damage than previous control groups.

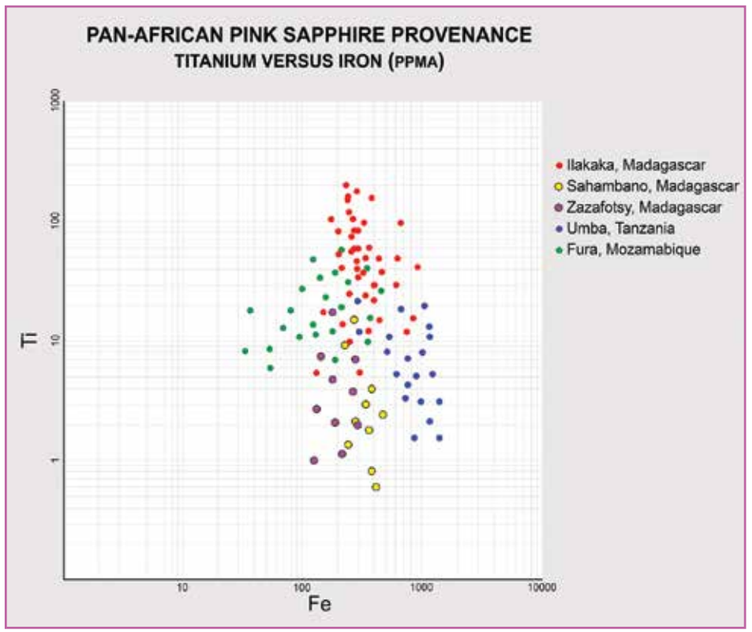

Figure 15. Titanium versus iron plotting of some Pan-African provenances. All the deposits have been selected for their presence of protogenetic zircons and overlapping trace elements with Ilakaka pink sapphires.

but no thermal-generated tension presented an FWHM superior to 11 (Figure 14).

Further sampling will be necessary for this potential criterion to be statistically relevant, as well as provide a better understanding of the tension formations for both cases and a statistical occurrence of said tensions in a pink sapphire before and after treatment at different heating conditions.

Focus on hypothesis assumptions and implications. In the opinion of the authors, the hypothesis followed for the low-heat treatment detection in Ilakaka pink sapphire assumes that, in finding the highest structural order naturally present in a zircon, one can assume that any zircon with a higher structural order will be the result of low-heat treatment. To apply the above hypothesis when receiving a gemstone in a laboratory, one must derive the conclusion from the following: We must presume we already know the origin and the deposit, that its zircon inclusions have a practical homogeneous amount of uranium and/or a similar age of formation, and that it was exposed to similar temperatures during their geological life within this deposit.

Assuming an Ilakakan origin, especially when very few laboratories write it on the origin determination of their report (understandable given the overlapping properties between other Madagascar deposits and other Pan-African orogeny origins, Figure 15), the authors believe that further study and research should be made to reduce the intrinsics risks of bringing such opposable results as the pillar from which heat treatment detection will be based upon, suggesting therefore, to include the validity and accuracy of most presented methods, as well as this one on the overlapping Pan-African deposits.

Conclusions

Based on the present study and a previous study (Zeug et al., 2016), the interpretation of v^3 peak position and FWHM by Raman spectroscopy on zircons of pink sapphire from Ilakaka, Madagascar include an important amount of false positives and false negatives as well as poor detection accuracy for most values at temperatures up to 1200°C. Should a value be used, it is based on this study, a FWHM equal or below 6 that offer the most conservative choice for an indication of heating, while a zircon with a tension and an FWHM value above 14 may be of potential use as a criterion for lack of thermal treatment and a value below 11 for an indication of tension resulting from low-heat treatment.

To conclude, using FTIR spectroscopy, careful visual observations, and the combination of the v^3 interpretation values proposed above as criterion yield a total low-heat treatment detection accuracy for the 31 heated samples of 97% with 0% false positives and one stone as a false negative.

Discussion

Focus on 3309 cm^{-1} coefficients. The notable decreased absorbance coefficient of the 3309 cm^{-1} after being heated (already noted by Saeseaw et al., 2020) deserves further research as a potential criterion for lack of treatment at low temperature.

Focus on heating due to the cutting process. The measured temperature of ~350°C from the heating necessary for the cutting process needs to be verified and controlled in a real-life scenario, as well as its implications, even if only for a few seconds on the potential hypothetical and practical consequences of such rapid and sometime repeated thermal shock on a zircon structure.

Focus on irradiation. Recent alerts and studies about potential artificial irradiation in corundum (Curti et al., 2022; Krzemnicki, 2023) and, more importantly, its indirect consequence on zircon inclusions might impact the relevance of any criterion in relation to a zircon structural order and should be investigated.

The 31 heated samples presented in this study as well as further unheated new references will be irradiated from 1 kGy to 2000 kGy using a ^{60}Co gamma-ray source to further understand the reliability and limitations of the presented criterion.

Acknowledgements

The authors are grateful to Theodore Rozet, Valentin Fejoz, Carolina Guzzi, Dr. Musilli, Dr.Guiliani, and Elsa Marlin for their numerous inputs, stimulating the discussions forward. Special thanks to Keevin Beneut and Etienne Balan who provided special assistance in the discussions as well.

About the Authors

M.P.H.Curti (martial@bellerophongemlab.com) is the founder and director of Bellerophon Gemlab Group, Paris, France. Hugo Ellia is a research scientist at Bellerophon Gemlab Thailand, Bangkok.

References

Balan. [202]. Theoretical infrared spectra of OH defects in corundum (α-Al2O3). *European Journal of Mineralogy*, Copernicus, 2020, 32 (5), pp.457-467. 10.5194/ejm-32-457-2020 . hal-02959747.

Beran A. [1991] Trace hydrogen in Verneuil-grown corundum and its colour varieties: An IR spectroscopic study. *European Journal of Mineralogy*, Vol. 3, No. 6, pp. 971–976, http://dx.doi.org/10.1127/ejm/3/6/0971.

Curti; Dr. Schwarz, Theodore Rozet, Hugo Ellia; [2022] Cautionary Note Corundum Irradiation Pre-Results induced amorphization of zircon through irradiation; 24.08.2022; https://www.gemlab analysis.com/_files/ugd/4dbf69_28e8c2318a39478682861b91c2801917.pdf

Dubinsky, E.V.; Stone-Sundberg, J.; Emmett, J.L. A [2020] quantitative description of the causes of color in corundum. *Gems & Gemology,* 2020, 56, 2–28.

Dunaigre [2006]; A study on the low temperature heat treatment of pink sapphires from Ilakaka (Madagascar); Gubelin Gemlab, June 2006.

Elmaleh, Susanne Theodora Schmidt, Stefanos Karampelas Klemens Link, Lore Kiefert, Annette Süssenberger, and André Paul [2008]; U-Pb Ages of Zircon Inclusions in Sapphires from Ratnapura and Balangoda (Sri Lanka) and Implications for Geographic Origin; *Gems & Gemology,* Spring 2019, Vol. 55, No. 1; Gem corundum deposits of Madagascar: A review; Ore Geology Reviews, 34 (2008) 134–154.

Emmett J.L., Dubinsky E.V., Hughes R.W., Scarratt K. [2017] Color, spectra & luminescence. In R.W. Hughes, Ed., *Ruby & Sapphire: A Gemologist's Guide, Bangkok*, pp. 107–163.

Garver [2002]; Discussion: "Metamictisation of natural zircon: accumulation versus thermal annealing of radioactivity-induced damage" by Nasdala et al. 2001 (*Contributions to Mineralogy and Petrology*, 141:125-144) Contrib Mineral Petrol (2002) 143: 756–757 DOI 10.1007/s00410-002-0379-0, 23 July 2002.

Hanchar and Hoskin [2003], Zircon volume 53, *Reviews in Mineralogy & Geochemistry*, Volume 53 2003; Mineralogical Society of America and Geochemical society.

Holland H. and Gottfried D. [1955] The effect of nuclear radiation on the structure of zircon. *Acta Crystal.,* 8, 291–300.

Karampelas, S.; Hennebois, U.; Mevellec, J.-Y.; Pardieu, V.; Delaunay, A.; Fritsch, E. [2023]; Pink to Purple Sapphires from Ilakaka, Madagascar: Insights to Separate Unheated from Heated Samples. Minerals, 2023, 13, 704. https://doi.org/10.3390/min13050704.

Krogh T. E. and Davis G. L. [1975] Alteration in zircons and differential dissolution of altered and metamict zircon. *Carnegie Inst. Wash. Yearb.,* 74, 619–623.

Krzemnicki [2018]. New research by SSEF studies methods for detecting low-temperature heated rubies from Mozambique. Press Release, Basel, Switzerland: September 12, 2018.

Krzemnicki, [2023 a]; new and additional criteria to detect low-t heated corundum; Facette, 2023.

Krzemnicki, [2023 b]; at the frontier of research: irradiation experiments on corundum; *Facette*, 2023

Marsellos and J.I. Garver [2010]; Radiation damage and uranium concentration in zircon as assessed by Raman spectroscopy and neutron irradiation; *American Mineralogist,* Volume 95, pages 1192–1201, 2010.

Meldrum, L. A. Boatner, W. J. Weber et R. C. Ewing, [1998] Radiation damage in zircon and monazite, *Geochimica et Cosmochimica Acta*, Vol. 62, no 14, 1er Juillet 1998, p. 2509-2520 (DOI 10.1016/S0016-7037(98)00174-4).

Nasdala, Christian L. Lengauer, John M. Hanchar, Andreas Kronz, Richard Wirth, Philippe Blanc, Allen K. Kennedy, Anne-Magali Seydoux-Guillaume; [2002]; Annealing radiation damage and the recovery of cathodoluminescence; *Chemical Geology,* 191 (2002) 121– 140.

Pabst A. [1952] The metamict state. *American Mineralogist*, 37, 137–157.

Pardieu V., Saeseaw S., Detroyat S., Raynaud V., Sangsawong S., Bhusrisom T., Engniwat S., Muyal J. [2015] Low temperature heat treatment of Mozambique ruby. *GIA Research News*, https://www.gia.edu/gia-news-research-low-temperature-heattreatment-mozambique-ruby.

Ragan, D. D., Gustavsen, R., and Schiferl, D., [1992]. Calibration of the ruby R1 and R2 Fluorescence shifts as a function of temperature from 0 to 600 K. *Journal of Applied Physics,* 72 (12), 5539-5544.

Rakotondrazafy, Gaston Giuliani, Daniel Ohnenstetter, Anthony E. Fallick, Saholy Rakotosamizanany, Alfred Andriamamonjy, Théogène Ralantoarison, Madison Razanatseheno, Yohann Offant, Virginie Garnier, Henri Maluski, Christian Dunaigre, Dietmar Schwarz, Voahangy Ratrimo, [2008]; Gem corundum deposits of Madagascar: A review; *Ore Geology Reviews,* 34 (2008) 134–154.

Saeseaw S., Kongsomart B., Atikarnsakul U., Khowpong C., Vertriest W., Soonthorntantikul W. [2018] Update on "low-temperature" heat treatment of Mozambican ruby: A focus on inclusions and FTIR spectroscopy. GIA Research News, https://www.gia.edu/ongoing-research/update-low temperature-heat-treatment-mozambican-ruby-focus-on-inclusionsand-ftir-spectroscopy.

Saeseaw; Khowpong, C. [2019]; The effect of low-temperature heat treatment on pink sapphire. *Gems & Gemology,* 2019, 56, 290–291.

Sripoonjan, T.; Wanthanachaisaeng, B.; Leelawatanasuk, T. [2016]; Phase Transformation of Epigenetic Iron Staining: Indication of Low-Temperature Heat Treatment in Mozambique Ruby. *J. Gemmology,* 2016, 35, 156–161.

Wang W, Kenneth Scarratt, John L. Emmett, Christopher M.Smith; Breeding, and Troy R. Douthit [2006]; The effects of heat treatment on zircon inclusions in Madagascar sapphires; *Gems & Gemology,* Vol. 42, No. 2, pp. 134–150; 2006.

Wanthanachaisaeng, B. [2007] The Influence of Heat Treatment on the Phase Relations in Mineral Growth Systems. Ph.D. Thesis, Johannes Gutenberg University of Mainz, Mainz, Germany, 2007; 79p.

Wong, W.C., McClure, D.C. et al. [1995 a] Charge-exchange processes in titanium-doped sapphire crystals. I. Charge-exchange energies and titanium-bound exitons. *Physical Review B*, Vol. 61, No. 9, pp. 5682–5692.

Wong, W.C., McClure, D.C. et al. [1995 b] Charge-exchange processes in titanium-doped sapphire crystals. II. Charge-transfer transition states, carrier trapping, and detrapping. *Physical Review B,* Vol. 61, No. 9, pp. 5693–5698.

Xu and Krzemnocki., [2021]; Wenxing Xu, Michael S. Krzemnicki; Raman spectroscopic investigation of zircon in gem-quality sapphire: Application in origin determination; *Raman Spectroscopy*, Volume 52, issue 5; May 2021.

Zhang, Y., [1998]. Mechanical and phase equilibria in inclusion-host systems. *Earth and Planetary Science Letters*, 157, pp. 209-222.

Zhang et al [2000]; Annealing of α-decay damage in zircon: a Raman spectroscopic study; Ming Zhang, Ekhard K H Salje, Gian Carlo Capitani, Hugues Leroux, Andrew M Clark, Jochen Schluter, and Rodney C Ewing; *J. Phys.: Condens. Matter*, 12 [2000] 3131–3148. 16 December 1999.

Zeug et al 2016; Spectroscopic study of inclusions in gem corundum from Mercaderes, Cauca, Colombia; Manuela Zeug1 - Andrés Ignacio Rodríguez Vargas2 - Lutz Nasdalal; *Phys. Chem. Minerals* (2017) 44:221–233 DOI 10.1007/s00269-016-0851-4.